Welding in the World (2018) 62:29–38
https://doi.org/10.1007/s40194-017-0530-1

RESEARCH PAPER

Mechanical manipulation of solidification during laser beam welding of aluminum

T. Radel[1]

Received: 21 July 2017 / Accepted: 15 November 2017 / Published online: 30 November 2017

Abstract
Mechanical vibrations affect the nucleation and grain growth conditions during solidification and are used as refinement method in the field of casting processes. This paper contributes to identify the influence of applied vibrations during laser beam welding of aluminum on the resulting grain structure. Therefore, it is investigated if the frequency amplitude factor, which suitably describes the grain refinement in casting processes, can be used to describe the grain refinement in laser deep penetration welding. The results show a local grain size reduction and an increase of the percentage of equiaxed grains due to applied excitation. A dependence of the resulting percentage of equiaxed grains on the product of frequency and amplitude cannot be observed within this study.

Keywords Grain size · Vibration · Microstructure

1 State of research

Solidification manipulation by applying additional vibrations is a common method in the field of metal casting to reduce the grain size and therefore to improve the mechanical properties of castings. The resulting microstructure strongly depends on the nucleation and grain growth conditions during casting which additional applied vibrations can affect. The number of nuclei depends on the nucleation conditions. On the one hand, nuclei can develop without any solid particles by homogeneous nucleation and, on the other hand, in the presence of solid particles by heterogeneous nucleation. The heterogeneous nucleation is influenced by dendrite fragmentation and grain detachment that affect the amount of solid particles for nucleation [1]. The dominating mechanism for dendrite fragmentation by excitation seems to be more likely root bending compared to root shearing or root remelting [2]. According to Hellawell et al. [3], the main reason for grain refinement is more likely the dispersion of dendrite fragments than its fragmentation itself assuming that enough fragments are present anyway. The reason for dendrite fragmentation in non-vibrated casting is driven by gravity-induced solute transport into the mushy zone as shown with x-ray in situ measurements by Ruvalcaba et al. [4].

The effectiveness of grain refinement depends on the applied vibration conditions. Campbell showed for casting processes that the product of excitation frequency and amplitude suitably describes the degree of grain refinement for several orders of magnitude of frequencies (approx. 10^0 to 10^5 Hz) and amplitudes (approx. 10^{-2} to 10^{-7} m) [2]. The possibility that an applied excitation can affect the solidification conditions during welding was shown for different kinds of welding processes and materials. The excitation can be applied to the workpiece or directly into the weld pool, or in the case of arc processes indirectly by molten droplet oscillation, welding arc oscillation, or electrode vibration [5]. Figure 1 gives an overview about the applied excitation frequencies and amplitudes in fusion welding processes with workpiece excitation at a certain frequency. The investigated weld seam properties in these experiments are very different including mechanical properties [6], porosity [7], residual stresses [8], and grain refinement [9]. Nevertheless, many of these properties are a result of refined grains. The filling color indicates if a positive impact on the investigated properties is observed (green) or

Recommended for publication by Commission IV - Power Beam Processes

✉ T. Radel
radel@bias.de

[1] BIAS - Bremer Institut für angewandte Strahltechnik GmbH, Klagenfurter Str. 5, 28359 Bremen, Germany

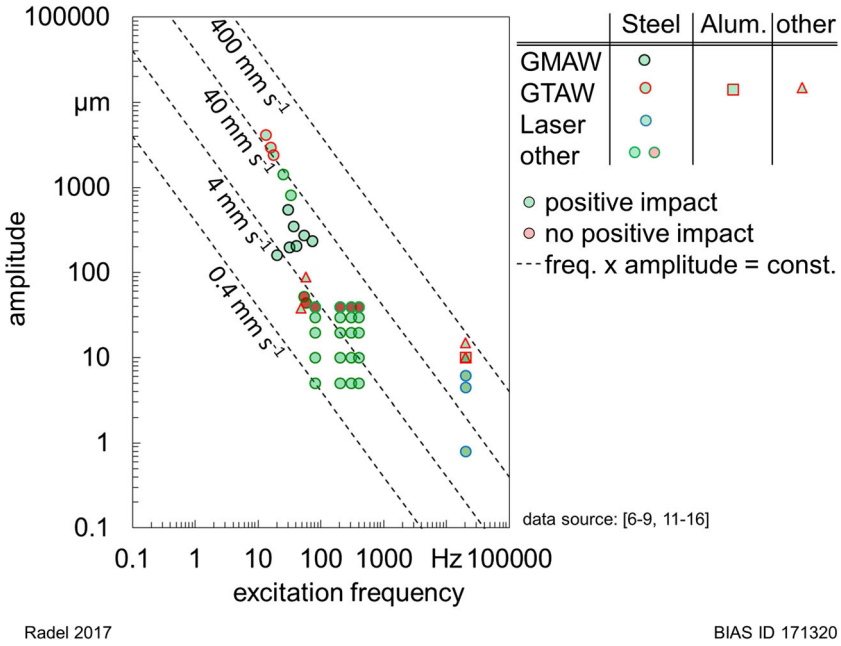

Fig. 1 Overview about fusion welding processes with a workpiece excitation at a certain frequency. The base material categories include their alloys; processes are categorized systematically: GMAW (gas metal arc welding) includes MIG (metal inert gas) and MAG (metal active gas) welding

not (red). Within these data, no relation is observed between the frequency and amplitude factor and the influence on the weld properties. It is noticeable that the number of published results without positive impact on the material properties is low. Woizeschke et al. [10] showed that grain refinement by mechanical vibrations during laser keyhole welding of aluminum alloy is generally possible.

2 Purpose

The state of research shows that the product of excitation frequency and amplitude is a suitable factor to describe the grain refinement in casting processes. However, the transferability of the frequency amplitude factor to describe the grain refinement in short-time processes like laser beam welding has not been investigated yet. The solidification and nucleation process in laser beam welding significantly differ from casting due to much higher temperature gradients and nucleation rates. Furthermore, the probability of fractured grains and dendrites to remain solid in the significantly overheated melt with high local thermal gradients is lower.

Based on the state of research, the following hypothesis is formulated: The frequency amplitude product is suitable to describe the extent of grain refinement in laser deep penetration welding of aluminum alloy. In order to test the hypothesis, this study investigates the influence of excitation frequency and amplitude on the resulting grain structure and distribution. Thereby, conclusions about the interaction between the solidifying melt and excitation should be drawn.

3 Experimental

3.1 Welding setup

A conventional laser optic (BEO D70 by Trumpf) which is connected to a multi-mode Yb:YAG (Ytterbium-doped yttrium aluminum garnet) disk laser (TruDisk 12002 by Trumpf) by a fiber of 200 µm core diameter was used. The optic contained a collimation lens with 200 mm focal length and a focusing lens with 200 mm focal length resulting in a nominal focal diameter of 200 µm. The focal plane was set 2.5 mm below the base material surface. Argon was applied as shielding gas on the top and bottom side. The experiments were carried out as full-penetration bead-on-plate welds. The weld path is linear and has been realized by a moving optic and a stationary specimen. Each set of parameters was carried out three times. The welding process parameters are summarized in Table 1.

Table 1 Applied welding parameters

Parameter	Value
Laser	Yb:YAG disk laser (Trumpf TruDisk 12002)
Wavelength	1030 nm
Nominal focal diameter	200 µm
Laser power	3.75 kW
Process velocity	4.0 m/min (66.7 mm/s)

3.2 Excitation setup

A digital function generator (HM8150 by Hameg instruments) was used as signal source. A power amplifier (PA500L by LDS - Ling Dynamic Systems) amplified the control signal. The amplified control signal leads to a one-directional motion of the electrodynamic shaker (V406 by LDS - Ling Dynamic Systems). The mass of the shaker armature was 0.2 kg. A clamping device with integrated channel for the root shielding gas was mounted at the top of the shaker and clamped the specimens at four points. An acceleration sensor (8714B500 by Kistler) was mounted in the middle of the specimen. The additional moving mass was 0.3 kg. The acceleration sensor used a piezoelectric measurement concept, according to the IEPE (Integrated Electronics Piezo Electric) industrial standard, based on the shear stresses. A signal conditioner (5118B2 by Kistler) was used as constant current source for the acceleration sensor and separated the measurement signal from the power signal. Further, a high-pass filter having a cutoff point of 0.03 Hz was included in the signal conditioner. A transient recorder (2580P by Gould Nicolet) measured the measurement signal of the acceleration and the signal created by the function generator with a frequency of 200 kHz and a recording time of 1.25 s. The experimental setup is given in Fig. 2a.

The function generator created sinusoidal control signals for the laser welding experiments. The accelerations were measured three times at each set of parameter and a sine fit was calculated for each measurement. The mean coefficient of determination R^2 of the sine fits was 0.989 ± 0.013. Based on this coefficient of determination R^2, the accelerations were described as a harmonic sinusoidal acceleration. The investigated matrix of max. accelerations and frequencies is given in Fig. 2b. In addition, welding without excitation was carried out as reference.

The amplitudes calculated by Eq. 1 for harmonic sinusoidal acceleration are given in Fig. 3. The dashed isolines represent constant excitation frequency amplitude products. The colors separate three areas according to the thresholds for vibration-assisted casting by Campbell [2]: optimum for grain refinement (green), possible grain refinement (yellow), and no grain refinement (red).

$$s = \frac{a_{\max}}{(2\,\pi\,f)^2} \tag{1}$$

3.3 Material

The laser welding experiments were performed with aluminum alloy AlMg4.5Mn (EN AW-5083) sheets in H111 temper condition. The measured chemical composition of the base material is given in Table 2. The sheet dimension was 60 mm × 50 mm × 5 mm. The rolling direction of base material was crosswise to the welding direction.

3.4 Weld seam characterization

Cross sections were taken in the middle of the seam's length, wet-ground using silicon carbide abrasive paper (grid up to P1200), polished with diamond-suspension (3 μm particle size), finished with aluminum oxide polish (0.04 μm particle size), electrolytically etched with tetrafluoroboric acid, and photographed with polarized light, according to the method of barker. According to McCartney's definition of grain

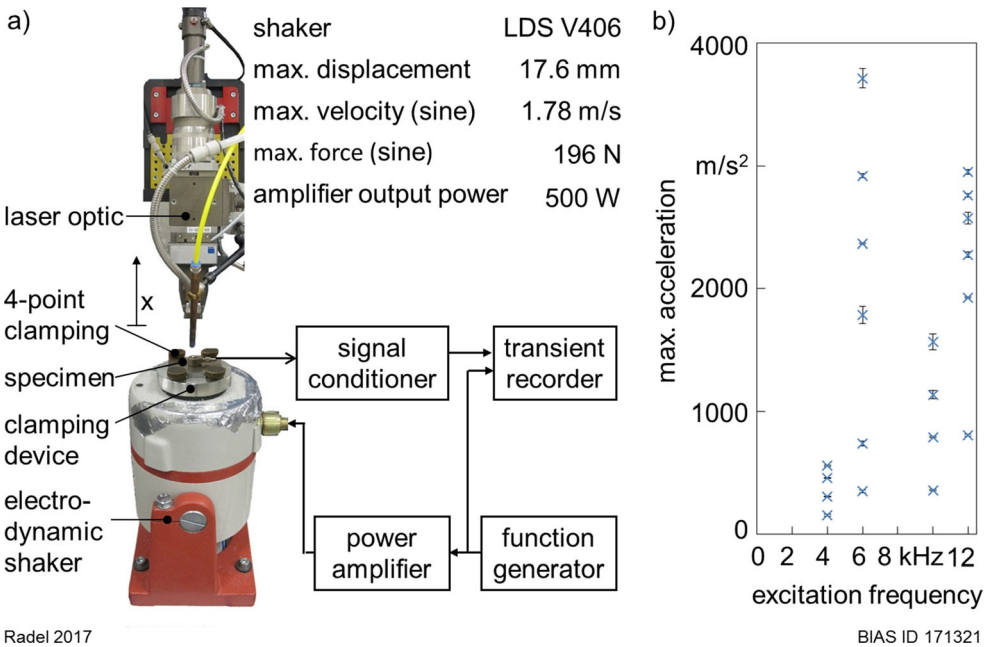

Fig. 2 **a** Experimental setup for welding with specimen excitation and **b** applied excitation parameters in the welding experiments

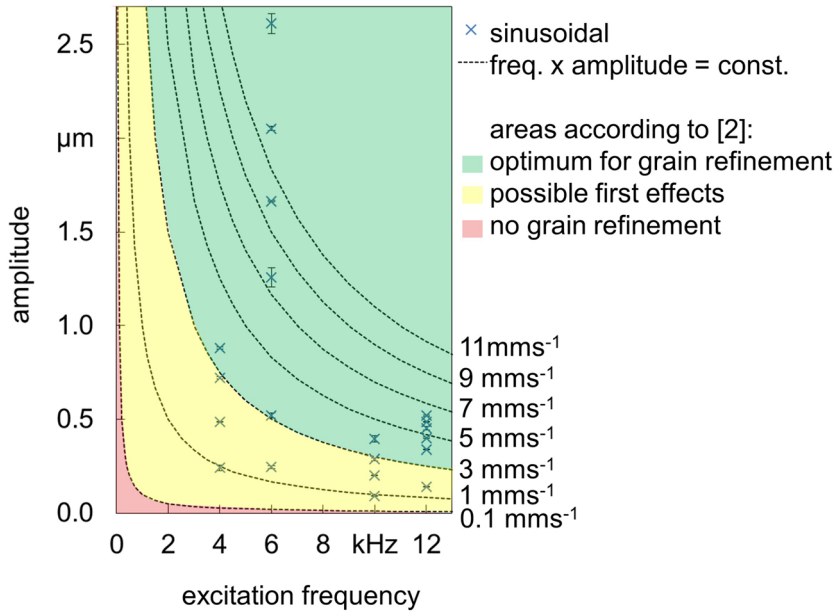

Fig. 3 Calculated amplitudes used in the welding experiments

refinement as the suppression of columnar grains [17], the percentage of equiaxed grains in the seam was used as a measure for grain refinement. The percentage of equiaxed grains in the seam was determined by determining the seam area and the area of equiaxed grains manually, Fig. 4. The distribution of the equiaxed grains is determined by using the MATLAB software, Fig. 4. Furthermore, the position of seam center point (given by blue and green areas in Fig. 4) and the center point of the area of equiaxed grains (given by green area in Fig. 4) were determined. The vector between these center points is calculated.

3.5 Estimating the interaction time between excitation and grain growth

The number of interactions n between a growing grain and the sinusoidal excitation was estimated by using the mean grain growth time. The solidification rate R depends on welding velocity v and the angle α between welding velocity v and solidification rate R that depends on the position in the seam:

$$R = v \times \cos(\alpha) \tag{2}$$

The angle α is between 0° and 90° depending on the position. In this estimation, the highest solidification rate R in the melt pool was used and therefore, the solidification rate R in the seam center was taken. In the case of high welding speeds and therefore tear-shaped weld pools, the angle α in the seam center remains larger than 0° as it is the case at low welding speeds with elliptical-shaped weld pools [18]. Therefore, the angle α at the seam center was determined. With the assumption that the dendrite and grain growth direction are similar,

Table 2 Measured chemical composition of the base material

Alloying element	Si	Fe	Cu	Mn	Mg	Cr	Zn	Ti	Al
Content in wt%	0.16	0.33	0.04	0.48	4.5	0.08	0.01	0.02	Bal.

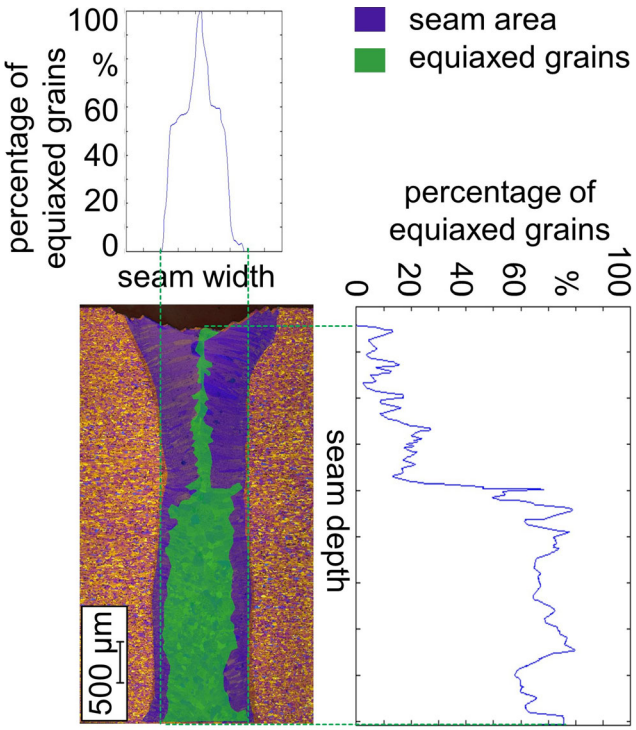

Fig. 4 Determination of the percentage of equiaxed grains in the seam and its distribution as a function of the width and depth

the angle α at the seam center was measured at ten positions at a topsectional view, according to [19].

The mean time of a growing grain t_{gr} is therefore given by the grain size s_g and the solidification rate R:

$$t_{gr} = \frac{s_g}{R} \tag{3}$$

The mean grain size of the non-vibrated specimens was therefore characterized by using circular intercept method [20] with three concentric cycles having a diameter of 214, 374, and 534 μm at four positions in the seam center. Thereby, a mean value is determined independently if these grains are columnar or equiaxed.

The number of interactions n between a growing grain and the excitation can therefore be described to the following:

$$n = t_{gr} \times f_{exc} \tag{4}$$

4 Results

The grain structure of the non-vibrated weld mainly consists of comparatively coarse columnar grains, Fig. 5a). Some equiaxed grains are located close to the seam centerline. Compared to the non-vibrated weld, the grain structure of the weld with applied vibration is finer and mainly consists of equiaxed grains, Fig. 5b).

The mean percentage of equiaxed grains is 28% in the case of non-vibrated specimens and between 26 and 62% in the case of excited specimen, Fig. 6. Nevertheless, the percentage of equiaxed grains is generally increased in the case of excited welds compared to that in the reference weld. The percentage of equiaxed grains does not show a clear trend with increasing frequency amplitude product. Moreover, no clear tendency is visible within a constant excitation frequency.

The distributions of the equiaxed grains in the case of 4, 6, 10, and 12 kHz excitation frequencies are given in Figs. 7, 8, 9, and 10, respectively. Compared to the non-vibrated reference weld, the percentage of equiaxed grains increases near the middle of the seam width. In the middle of the seam width, the percentage of equiaxed grains increases up to 100%. In the case of an increased percentage of equiaxed grains at 6 and 10 kHz (compare Fig. 6), the increase takes place in the lower area of the seam cross section, Figs. 8 and 9. The percentage of equiaxed grains in the upper 40% of the weld does not show a clear increase due to the excitation.

The relative position of center point of the area of equiaxed grains compared to that of the center point of the seam area is given in Fig. 11. Similar center points would result in position (0, 0). The mean center point of the non-vibrated weld and in the case of all excited welds is below the seam center point. The relative position shows no tendency related to the excitation frequency.

The mean angle α between welding velocity v and solidification rate R is determined for the non-vibrated reference weld at the seam center to 53°. With this value, the mean grain size of the non-vibrated reference weld (58 μm), the process parameter given in Table 1, and the assumptions in the "Estimating the interaction time between excitation and grain growth" section, the number of interaction cycles between a growing grain in the

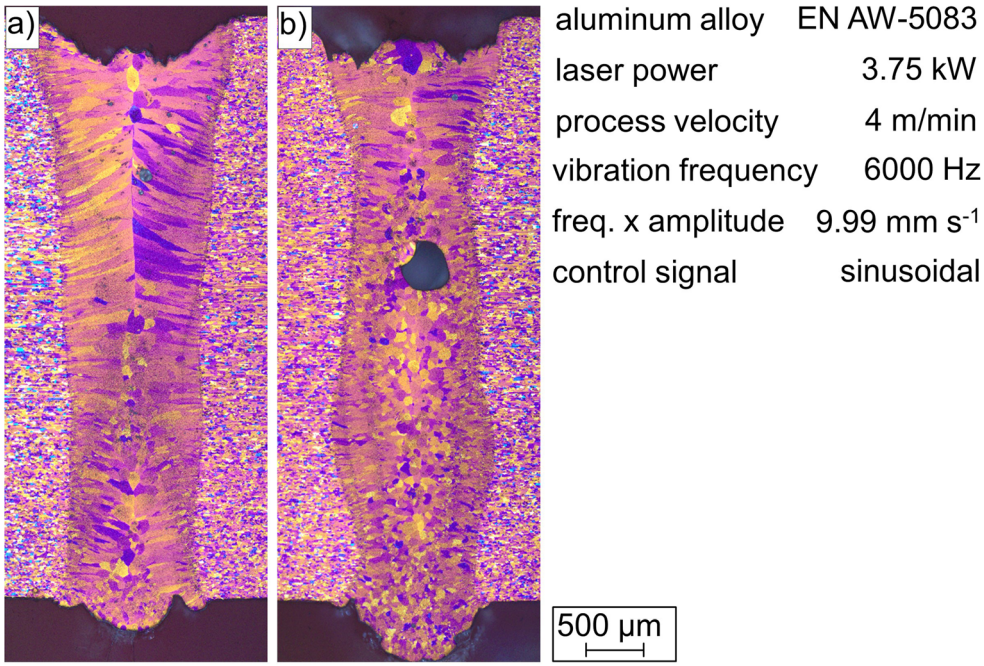

Fig. 5 Seam cross sections: **a** non-vibrated and **b** with vibration

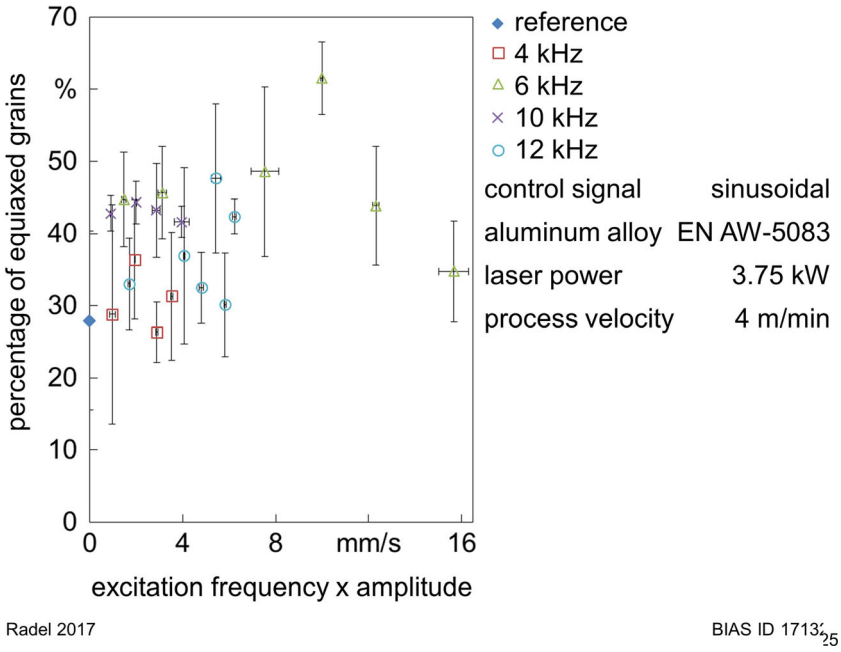

Fig. 6 Measured percentage of equiaxed grains for different products of frequency and amplitude

excitation are calculated by using Eqs. 2, 3, and 4. The estimation leads to 5.8 and 17.4 interaction cycles between the averaged grain growth time and the excitation in the case of an excitation frequency of 4 and 12 kHz, respectively.

5 Discussion

The results of the non-vibrated welds show a low percentage of equiaxed grains, which are primarily located in the seam center. According to the state of research, the non-vibrated weld seam should be solidified by the following mechanism: The grains start growing at the fusion line—in fusion welding without filler wire—in epitaxial direction [1]. The grains grow further in the so-called competitive growth [1]. Thereby, in the seam center, equiaxial grains occur in the case of high welding speeds and heat input. These equiaxial grains seem to be built by heterogeneous nucleation which is assisted by constitutional undercooling [21] and occlude growing of columnar grains [22]. By applying workpiece excitations, the percentage of equiaxed grains is generally increased, Fig. 6. Hence, the application of workpiece excitations leads to a transition from

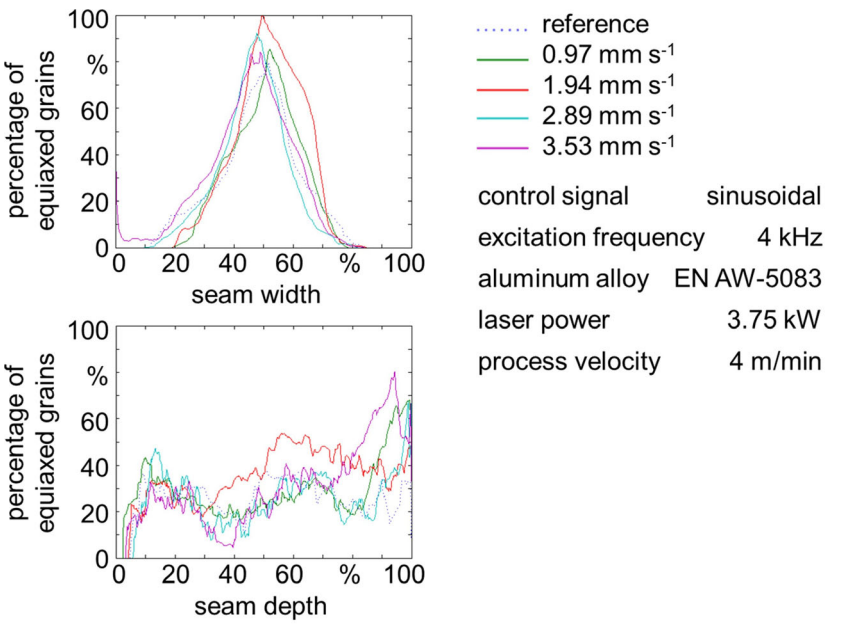

Fig. 7 Distribution of the equiaxed grains in the seam width and depth at an excitation frequency of 4 kHz

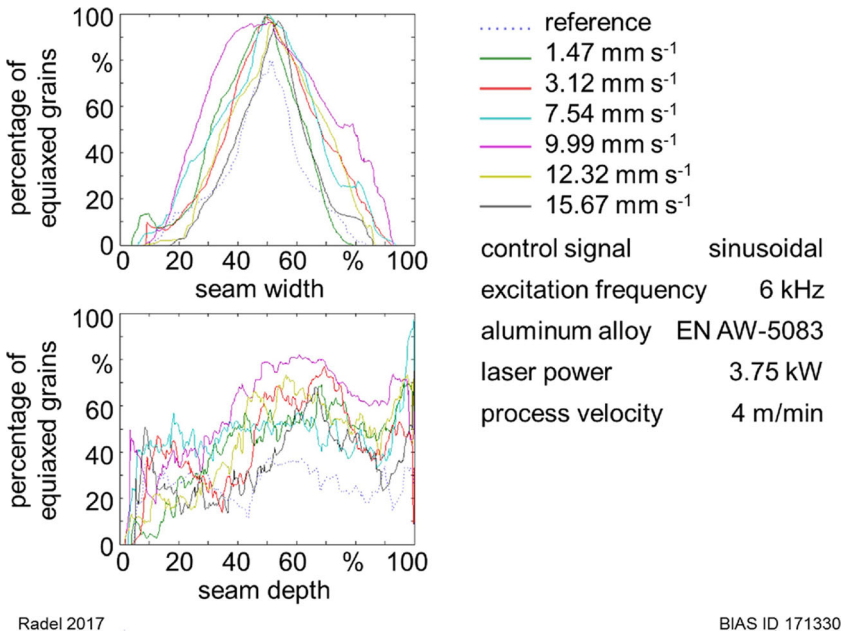

Fig. 8 Distribution of the equiaxed grains in the seam width and depth at an excitation frequency of 6 kHz

columnar to equiaxed grains. This is in line with the results for gas tungsten arc welding in [23]. The transition from columnar to equiaxed grains is an indication of an increased number of solid particles for heterogeneous nucleation that lead to a domination of equiaxed grains during the competitive growth. Independently, if the number of solid particles is increased by fractured grains or dendrites or if it is a result of dispersion of particles, it can be concluded that particles can remain solid and act therefore as nuclei for grain nucleation in the given conditions of laser deep penetration welding of aluminum which is typically characterized by significantly overheated melt and comparatively high local thermal gradients. The number of equiaxed grains in the non-vibrated reference weld is too small to apply linear or circular intercept methods to reliably determine the grain size of the equiaxed grains. Therefore, further investigations are necessary in order to evaluate if applied excitation also affects the size of equiaxed grains.

The grain structure differs along the seam depth, Fig. 7. The solidification conditions depend on the position in the seam in two ways: the thermal behavior according to the thermal gradient G and growth rate R and the geometrical interactions between solidifying melt and excitation. The seams show a nearly constant seam width in depth

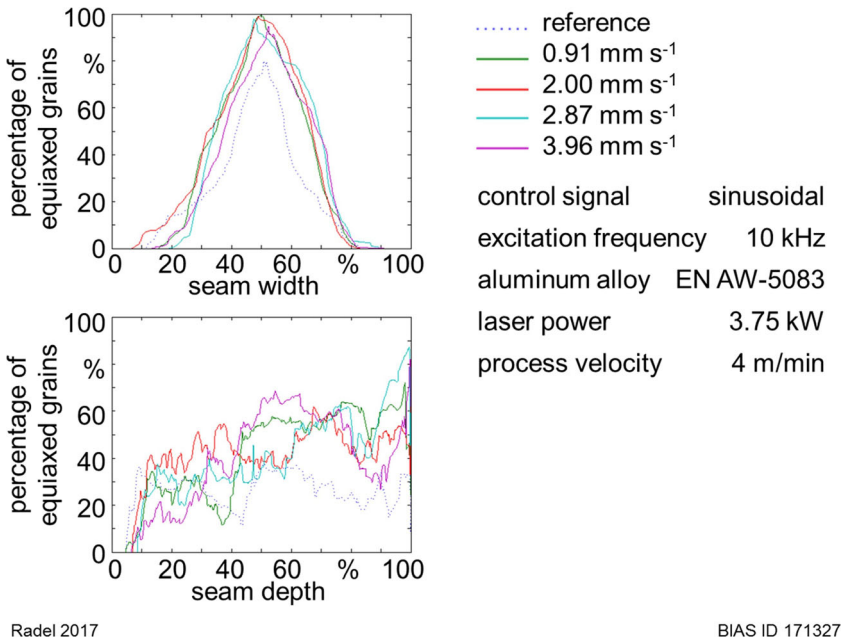

Fig. 9 Distribution of the equiaxed grains in the seam width and depth at an excitation frequency of 10 kHz

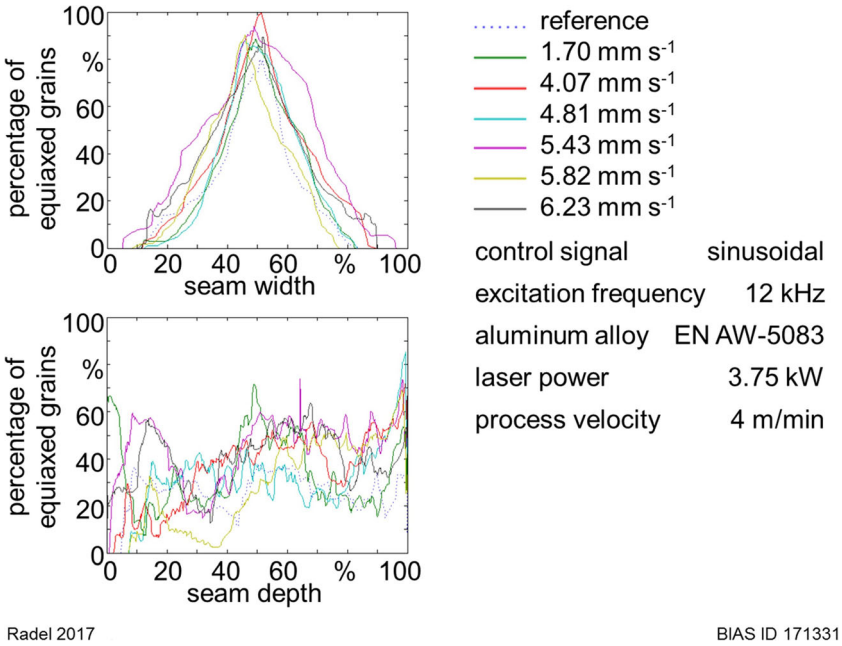

Fig. 10 Distribution of the equiaxed grains in the seam width and depth at an excitation frequency of 12 kHz

direction, compare Fig. 4. Therefore, the angle between epitaxial (nearly horizontal) growing grains and one-directional excitation is not significantly depending on the depth. There seems to exist no favorable area for fragmentation according the theory of fragmentation by shearing or bending. This distinguishes this weld seam from those given in [10], where also a less efficient refinement is observed in the upper area of the v-shaped seams. The results show that the center point of equiaxed grains is below the center point of the seam in the non-vibrated reference weld and in all excited welds, Fig. 11. There seems to be favorable thermal conditions for equiaxed grains compared to the upper seam area. A finer grain size and an increased percentage of equiaxed grains in the lower seam have also been observed in other laser aluminum welds, e.g., AA 8090 as shown in [24] and in the case of welding with workpiece excitation [10]. According to Whitaker, the equiaxed grains in the lower seam area probably result by favorable local fluid and heat flow conditions [24]. The increase of the percentage of equiaxed

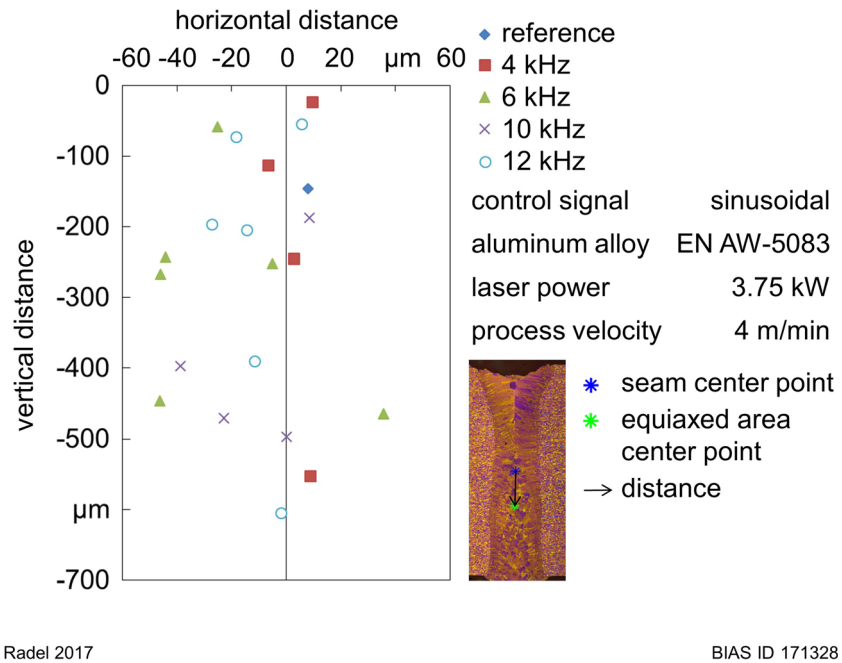

Fig. 11 Position of center point of the equiaxed area compared to the seam center point

grains primary take place in the lower area of the seam, Figs. 8 and 9. This extends the state of research compared to the results given in [10] where a location depending grain refinement is shown for excitation parameters below the optimum range, compare Fig. 3. Thus, the location dependency also exists at excitation parameters that are in the described optimum range. If this increase of equiaxed grains in the lower area of the seam is primary based on favorable thermal conditions, or if the melt pool excitation is less efficient in the upper area due to the already solidified root, it cannot be separated in this investigation.

Feng-Quan and Xiao-Ling [25] showed the impact of vibration and shock affects the solidifying melt only in the close vicinity of the solid-liquid interface. Thus, a too low excitation frequency could result in a nonuniform manipulation of the solidifying melt. In order to understand the interaction between solidifying melt and excitation, the number of interaction cylces n between the growing time of a grain and the excitation is estimated ("Results" section). The fact that each growing grain undergoes more than one complete sine excitation cycle is an indicator that the applied frequencies are generally high enough to fulfill the conditions for uniform manipulation based on the fact that the excitation affects only the close vicinity of the solid-liquid interface as shown by Feng-Quan and Xiao-Ling [25]. Therefore, the applied excitation frequency range (4 till 12 kHz) cannot explain the deviation from the expected behavior that the grain refinement will be more extensive with increasing frequency amplitude product. According to the classification by Campbell [2] for casting processes, the applied excitation frequency amplitude products are in the ranges for possible first effects and optimum for grain refinement. The percentage of equiaxed grains does not show a clear dependence on the excitation frequency amplitude product. The thesis that the frequency amplitude product can describe the extent of grain refinement in laser deep penetration welding of aluminum alloy can therefore not be confirmed by the results in the investigated range between 0.91 and 15.67 mm s^{-1}. McInerney et al. determined the threshold for grain refinement during gas tungsten arc welding of aluminum alloy 2219 to 19 mm s^{-1} [23]. This threshold is higher than the applied excitations within this study and higher compared to the lower threshold for casting processes. The solidification and nucleation conditions in (laser-) welding significantly differ from casting due to higher temperature gradients and nucleation rates and may lead to different requirements for mechanical manipulation of solidification. Furthermore, the laser deep penetration welds are characterized by their narrow width (compare Fig. 5) which may be disadvantageous for the excitation of the melt. Therefore, further investigation needs to evaluate if wider melt pools are advantageous for grain refinement during laser deep penetration welding.

6 Conclusion

The results of the study on the influence of mechanical solidification manipulation during laser deep penetration welding of aluminum are summarized as follows:

- Applying a workpiece excitation during laser deep penetration welding of aluminum alloy EN AW-5083 leads to a transition from columnar to equiaxed grains.
- The results do not show a trend of the percentage of equiaxed with respect to the product of excitation frequency and amplitude. Thus, it cannot be confirmed for the investigated parameter range that the frequency amplitude product is, besides casting, also applicable to describe the extent of grain refinement in laser deep penetration welding of aluminum alloy EN AW-5083.

Acknowledgements This work was accomplished within the Center of Competence for Welding of Aluminium Alloys – CentrAl. Funding by the Deutsche Forschungsgemeinschaft DFG (VO 530/85-1) is gratefully acknowledged. The author also thank A. Derksen for performing the experiments during his bachelor thesis.

References

1. Kou S (2003) Welding metallurgy. Wiley Inc, Hoboken
2. Campbell J (1981) Effects of vibration during solidification. Int Met Rev 2:71–108
3. Hellawell A, Liu S, Lu Z (1997) Dendrite fragmentation and the effects of fluid flow in castings. JOM 49(3):18–20. https://doi.org/10.1007/BF02914650
4. Ruvalcaba D, Mathiesen RH, Eskin DG, Arnberg L, Katgerman L (2007) In situ observations of dendritic fragmentation due to local solute-enrichment during directional solidification of an aluminum alloy. Acta Mater 55(13):4287–4292. https://doi.org/10.1016/j.actamat.2007.03.030
5. Jose MJ, Kumar SS, Sharma A (2016) Vibration assisted welding processes and their influence on quality of welds. Sci Technol Weld Join 21(4):243–258. https://doi.org/10.1179/1362171815Y.0000000088
6. Tewari SP, Shanker A (1994) Effects of longitudinal vibration on the mechanical properties of mild steel weldment. Proc Inst Mech Eng Part B J Eng Manuf 207:173–177
7. Krajewski A, Włosiński W, Chmielewski T, Kołodziejczak P (2012) Ultrasonic-vibration assisted arc-welding of aluminum alloys. Bull Pol Acad Sci Tech Sci 60:841–852
8. Aoki S, Nishimura T, Hiroi T, Hirai S (2007) Reduction method for residual stress of welded joint using harmonic vibrational load. Nucl Eng Des 237(2):206–212. https://doi.org/10.1016/j.nucengdes.2006.06.004
9. Gericke A, Banaschik R, Henkel K-M (2015) Zähigkeitserhöhung durch Schmelzbadvibration UP–geschweißter Feinkornbaustähle. Tagungsband DVS–Berichte 315:695–700 (in german)
10. Woizeschke P, Radel T, Nicolay P, Vollertsen F (2017) Laser deep penetration welding of an aluminum alloy with simultaneously applied vibrations. Lasers Manuf Mater Process 4(1):1–12. https://doi.org/10.1007/s40516-016-0032-9

11. Govindarao P, Srinivasarao P, Gopalakrishna A, Sarkar MMM (2012) Effect of vibratory welding process to improve the mechanical properties of butt welded joints. Int J Mod Eng Res 2: 2766–2770
12. Methong T, Poopat B (2013) The effect of ultrasonic vibration on properties of weld metal. Key Eng Mater 545:177–181. https://doi.org/10.4028/www.scientific.net/KEM.545.177
13. Qinghua L, Ligong C, Chunzhen N (2008) Effect of vibratory weld conditioning on welded valve properties. Mech Mater 40(7):565–574. https://doi.org/10.1016/j.mechmat.2007.11.001
14. Sakthivel P, Sivakumar P (2014) Effect of vibration in Tig and arc welding using AISI 316 stainless steel. Int J Eng Res Sci Technol 3: 116–130
15. Venkannah S, Mazumder J (2009) Changes in laser weld bead geometry with the application of ultrasonic vibrations. In: Ao SI, Gelman L, Hukins DWL, Hunter A, Korsunsky AM (eds) Proceedings of the World Congress on Engineering Vol II. London, pp 1612–1617
16. Wu W (2000) Influence of vibration frequency on solidification of weldments. Acta Metall 42:661–665
17. McCartney DG (1989) Grain refining of aluminium and its alloys using inoculants. Int Mater Rev 34(1):247–260. https://doi.org/10.1179/imr.1989.34.1.247
18. David SA, Vitek JM (1989) Correlation between solidification parameters and weld microstructures. Int Mater Rev 34(1):213–245. https://doi.org/10.1179/imr.1989.34.1.213
19. Schempp P, Rethmeier M (2015) Understanding grain refinement in aluminium welding. Weld World 59(6):767–784. https://doi.org/10.1007/s40194-015-0251-2
20. Vander Voort GF (1984) Metallography, principles and practice. McGraw-Hill Book Co., NY ASM International
21. Ganaha T, Pearce BP, Kerr HW (1980) Grain structures in aluminum alloy GTA welds. Metall Trans A 11(8):1351–1359. https://doi.org/10.1007/BF02653489
22. Kou S, Le Y (1988) Welding parameters and the grain structure of weld metal—a thermodynamic consideration. Metall Trans A 19(4):1075–1082. https://doi.org/10.1007/BF02628392
23. McInerney TJ, Madigan RB, Xu P, Cross CE (2006) Achieving grain refinement through weld pool oscillation. In: David SA, DebRoy T, Lippold, JC, Smartt HB, Vitek JM (eds) Trends in welding research: Proceedings of the 7th International Conference. ASM International, pp 17–22
24. Whitaker IR, McCartney DG, Calder N, Steen WM (1993) Microstructural characterization of CO_2 laser welds in the Al-Li based alloy 8090. J Mater Sci 28(20):5469–5478. https://doi.org/10.1007/BF00367817
25. Feng-Quan W, Xiao-Ling H (2000) The influence of vibration & shock on the crystal growth during solidification. J Mater Sci 35(8): 1907–1910. https://doi.org/10.1023/A:1004758217149